Journal of Experimental Marine Biology and Ecology 587 (2025) 152103

Contents lists available at ScienceDirect

Journal of Experimental Marine Biology and Ecology

journal homepage: www.elsevier.com/locate/jembe

# A DNA-based investigation of endolithic community succession on shells of the limpet *Patella depressa* Pennant 1777

Adam J. Wyness [a,b], Mauricio Oróstica [a,c], Jonathan R. Monsinjon [a,d], Christopher D. McQuaid [a,*]

[a] Coastal Research Group, Department of Zoology and Entomology, Rhodes University, Grahamstown, 6140, South Africa
[b] Scottish Association for Marine Science, Dunbeg, OBAN, PA34 1QA, UK
[c] Centro de Investigación de Estudios Avanzados del Maule (CIEAM), Vicerrectoría de Investigación y Postgrado, Universidad Católica del Maule, Talca, Chile
[d] Institut Français de Recherche pour l'Exploitation de la Mer (IFREMER), Délégation Océan Indien (DOI), Rue Jean Bertho, Le Port, La Réunion BP 60 – 97822, France

ARTICLE INFO

*Keywords:*
Bioerosion
Euendolith
Lithobiont
Ocean acidification
Microbiome
Rocky shore

ABSTRACT

Biotic and abiotic calcium carbonate structures are used as a substrate by bioeroding organisms, or euendoliths, worldwide. Euendoliths can have serious ecological effects on living hosts, and with global increases in ocean acidification and warming, the efficiency of erosion by marine euendoliths is likely to increase. Here, we used growth curve data for the limpet *Patella depressa* and 16S rRNA sequencing to explore succession in the endolithic community on the shells of *P. depressa* throughout its range across Great Britain. Limpet age correlated well with the extent of erosion within sites, but differed among sites, with those at the centre of the host range showing greater erosion when corrected for age. Alpha-diversity and richness of cyanobacteria decreased with the extent of erosion, particularly during the earlier stages of erosion. A decrease in the accumulation rate of Amplicon Sequence Variants (ASVs) occurred at around 80 % of cumulative ASVs, at a shell age of between 1.4 and 2.7 years. Cyanobacterial community composition differed among the shells from the different sites, but despite these differences, there were no discernable patterns in the abundance of specific taxa that were associated with limpet age or the extent of erosion. The results revealed that, when examined at a high taxonomic resolution, cyanobacterial community succession is more complex than previously thought, and may be site-specific. However, the trends observed indicate that cyanobacterial community succession occurs on calcifying organisms *in vivo*, with a shift towards a climax community after 1.4–2.7 years for *P. depressa*.

## 1. Introduction

Euendoliths are bioeroding organisms that include fungi, sponges, cyanobacteria and algae (Gektidis et al., 2007; Murphy et al., 2016; Gleason et al., 2017). They form part of the lithobiontic community, organisms that live on(epilithic) and in (endolithic) the substratum, and include chasmoendoliths and cryptoendoliths that inhabit previously eroded fissures and structural cavities, as well as epiliths that dwell upon the surface of the substratum (Golubic et al., 1981). Euendoliths, in contrast, are effective at excavating both biotic and abiotic calcium carbonate substrata, including the shells of molluscs and corals (Campbell, 1983; Campion-Alsumard and Hutchings, 1995; Kaehler, 1999; Pernice et al., 2020).

Bioerosion by euendoliths is ecologically important in the rocky intertidal zone where many ecologically key species produce calcified shells, so that components of the rocky shore ecosystem that depend on these key organisms are vulnerable to changes in the effects of euendoliths, particularly their bioerosive efficiency. Euendoliths have direct effects on the energy balance of hosts, increasing the need for shell repair and maintenance, thus reducing reproductive output and scope for growth over time (Kaehler and McQuaid, 1999; Day et al., 2000; Zardi et al., 2009; Ćurin et al., 2014; Ndhlovu et al., 2021). Shell erosion increases vulnerability to predation and disease, and can be the cause of up to 60 % of mortality of intertidal mussels due to shell collapse (Webb and Korrûbel, 1994; Kaehler and McQuaid, 1999; Gleason et al., 2017). Bioerosive decay of calcium carbonate is also, however, an important mechanism in both local (*e.g.*, near-shore communities and coral reefs) and global biogeochemical and nutrient cycling (Schneider and Le Campion-Alsumard, 1999; Tribollet et al., 2008; Pfister et al., 2010; Gleason et al., 2017), while phototrophic euendoliths are also significant

* Corresponding author at: Coastal Research Group, Department of Zoology and Entomology, Rhodes University, Grahamstown 6140, South Africa.
*E-mail address:* c.mcquaid@ru.ac.za (C.D. McQuaid).

https://doi.org/10.1016/j.jembe.2025.152103
Received 16 January 2025; Received in revised form 5 April 2025; Accepted 7 April 2025
Available online 10 April 2025

primary producers (Tribollet et al., 2006). The rate of euendolithic bioerosion is influenced by physical and chemical environmental conditions, including light intensity, temperature, nutrient level and ocean pH, but also varies among cyanobacterial species (Tribollet et al., 2009; Carreiro-Silva et al., 2012; Schönberg et al., 2017). Little is known about the colonisation and succession dynamics of euendolithic communities or how this relates to the degree of shell erosion.

Calcifying intertidal molluscs have a periostracum, a proteinaceous outer layer of the shell that allows the compartmentalisation of extrapallial fluid and synthesis of the calcium carbonate shell matrix. It remains on the outer surface of the shell as the organism grows, providing protection from both chemical and biological fouling (Wahl et al., 1998; Bers et al., 2006a, 2006b, 2010). Euendoliths excavate calcium carbonate by pumping calcium ions away from the substratum surface to create an increased dissolution gradient (Garcia-Pichel et al., 2010; Ramírez-Reinat and Garcia-Pichel, 2012; Guida and Garcia-Pichel, 2016), therefore the periostracum needs to be damaged or removed before euendoliths can colonise the calcium carbonate portion of the shell (Kaehler, 1999; Prusina et al., 2015). Several mechanisms can compromise the integrity of the shell by damaging or removing the periostracum, including abrasion by wave-suspended sediments, and grazing by other organisms, making the shell vulnerable to euendolithic infestation. Removal of the periostracum is followed by the erosion of the calcium carbonate layers, exposing the nacreous layers beneath. Therefore, when virgin calcium carbonate is exposed, there is likely to be succession of the euendolithic community on this new resource or habitat, with excavation by pioneer species creating further niches for other species to colonise and reach a stable community composition.

Evidence of succession of cyanobacterial euendoliths has been observed on intertidal species where the periostracum had been artificially removed to expose fresh calcium carbonate substratum (Ndhlovu et al., 2021). Based on morphological identification of euendolithic species on the mussels *Perna perna* and *Mytilus galloprovincialis*, cyanobacterial richness increased up to a total of six species after 9 months, with sampling finishing after 12 months when a stable community was observed. High throughput sequencing has also been used to observe euendolith community succession on abiotic carbonates (Roush and Garcia-Pichel, 2020). For example, on fresh travertine tiles, after 9 months cyanobacterial biomass and species diversity were similar to nearby climax communities. However, in that study, in contrast to that of Ndhlovu et al. (2021) there was no significant change in species richness, and species evenness and diversity decreased with time. In terms of euendolith community succession on shells, these studies were of relatively short duration compared to the host lifespan. Communities of lithobiontic cyanobacteria have been shown to differ among species and localities in relatively close proximity (Wyness et al., 2022a), but share common features on more global scales (Wyness et al., 2022b). Euendoliths may exhibit different preferences among substrata with different mineralogical compositions (Couradeau et al., 2017) and, as the shell erodes, there are chemical and microtopographical changes between the shell layers (Langer et al., 2014) that affect the ability of different species to colonise and compete, subsequently affecting the later composition of the euendolith community.

On the rocky shores worldwide, patellid limpets have a key role in controlling algal communities by grazing (Branch, 1981; Hawkins et al., 2008). In northwest Europe, the warm-water limpet species *Patella depressa* is one of the most conspicuous grazers at mid-shore levels at semi-exposed and exposed shores. It is distributed from North Africa to the British Isles (Moore et al., 2007; Oróstica et al., 2020), with two separate poleward edges in north Wales and in south-east England and with central populations in south-west England. It has been used as model organism to investigate shell growth patterns, enabling the estimation of its lifespan across its range (García-Escárzaga et al., 2020; Oróstica et al., 2021). Patterns of growth, mortality and age of *P. depressa* have recently been recorded between the two poleward limits, and historical records reveal an expansion of its distribution since the 1950s, with higher abundances at its eastern limit compared to populations at the Northern extent of its distribution. In addition, analysis of age patterns of limpets has shown that long-lived individuals (~10 years) (Oróstica et al., 2021) at northern latitudes in North Wales have slower shell growth patterns than individuals further south in Portugal (Silva et al., 2003). Overall, the existing studies of euendolithic community succession on marine habitats are of relatively short duration (months) when compared to the lifespan of key intertidal species such as limpets (> 10 years). Therefore, understanding succession of euendoliths and their longer-term effects on calcifying organisms requires insights into euendolith community change over periods that are aligned with the lifespans of the host organisms.

In this study, we examined how endolithic communities change with the age of the host *Patella depressa*. To do this, the composition of the cyanobacterial endolithic community was examined *in vivo* by sampling progressively older bands of limpet shells, using previously obtained growth curve data to estimate the age of each band. This allowed three hypotheses to be tested: 1) Age is a good indicator of shell erosion. The age and degree of erosion of the shell could then be used as factors to assess the other hypotheses: 2) endoliths exhibit community succession *in vivo*, and 3) endolithic community succession in *P. depressa* shells is uniform across the host's natural range, indicating that it is roughly deterministic.

## 2. Methods

### 2.1. Sampling of Patella depressa

Twelve adult specimens of *P. depressa* were collected from each of three locations in the United Kingdom: mid-range Polzeath (50°34′28.4"N, 4°55′13.6"W) in south-west England and the two range edges, Shell island in north Wales (52°49′11.2"N, 4°08′41.5"W) and Swanage in south-east England (50°36′27.0"N, 1°56′36.9"W, Table 1). For each shell, lithobiont samples were taken from areas of the shell in three concentric bands (2 mm wide). These were positioned (1) towards the apex of the shell (oldest), (2) in the middle, and (3) near the growing edge (newest), and measurements were taken of the shell diameter at each sampling band. Samples were taken by milling the shell surface to a depth of 1 mm of shell using a 3-mm diamond ball burr attachment on a rotary hand tool (Dremel Multi-tool 3000, Dremel, USA), with the resulting fine particulate matter (~10 mg) collected on foil and transferred to a centrifuge tube filled with 500 μl 100 % ethanol. Although older shells were clearly more eroded, supporting the first hypothesis, this was not consistent among sites, and so, instead of using age as a continuous variable, we used subjective evaluation of the degree of erosion in a factorial analysis. Shells were assigned a degree of erosion at each sampling point using an arbitrary scale: 0 = no sign of erosion, periostracum intact, 1 = periostracum eroded and calcium carbonate exposed, 2 = significant erosion of calcium carbonate layers, 3 = extensive erosion of calcium carbonate layers and underlying nacreous layers exposed. Each shell was evaluated this way by three independent researchers with the mean of these values used in further analyses. It is important to note that this sampling methodology results in the inclusion of all lithobionts present on the shell (Golubic et al., 1981).

### 2.2. Determination of the age of shell bands sampled

Previously published Von Bertalanffy Growth curve parameters for *P. depressa* at each of the sampling sites (Oróstica et al., 2021) were used to calculate the age of each of the bands on each shell where the lithobiont community was sampled (Table 2).

### 2.3. DNA extraction

DNA from the milled shell material was extracted using a phenol–chloroform extraction (Hogan et al., 1986) with modifications. Briefly,

**Table 1**
Site locations and Sea Surface Temperatures (SST) calculated using daily records from between 2017-08-01 and 2020-07-31.

| Site | Date Sampled | Latitude | Longitude | 3 year mean (°C) | 3 year median (°C) | 3 year upper quartile (°C) | 3 year lower quartile (°C) |
|---|---|---|---|---|---|---|---|
| Swanage | 09/09/2020 | 50.607067 | −1.944365 | 13.0 | 12.6 | 16.5 | 9.5 |
| Polzeath | 02/08/2020 | 50.573951 | −4.922478 | 13.0 | 12.6 | 15.9 | 10.1 |
| Shell Island | 09/08/2020 | 52.833539 | −4.128057 | 11.8 | 11.6 | 15.1 | 8.3 |

**Table 2**
Von Bertalanffy growth parameters used to calculate the age of each of the bands sampled on each shell. Where L max = the maximum length, L∞ = theoretical maximum the species can reach at the particular site, K = the rate at which the maximum size can be reached, T(0) = theoretical age at zero length, Ø' = growth performance index (Ø' = log K + 2log L∞).

| Site | L max (mm) | $L_\infty$ (mm) | K (years $^{-1}$) | $T_{(0)}$ | Ø' |
|---|---|---|---|---|---|
| Swanage | 34.5 | 37.4 | 0.269 | −0.247 | 2.58 |
| Polzeath | 36.5 | 40.1 | 0.191 | −0.866 | 2.49 |
| Shell Island | 33.9 | 34 | 0.214 | −0.994 | 2.29 |

samples were digested in 1.5 ml centrifuge tubes in 500 µl of lysis buffer (50 mM Tris–HCl pH 8.0, 100 mM EDTA pH 8.0, 100 mM NaCl, 0.5 % SDS) and 12.5 µl of proteinase K (10 mg/ml) at 56 °C for 12 h. An equal volume (500 µl) of phenol:chloroform:isoamyl alcohol (25:24:1) was added, and the solution vortexed for 1 min before centrifugation at 16,000*g* at room temperature. Up to 200 µl of the aqueous phase was transferred to a new centrifuge tube, and the centrifugation and transfer repeated to remove residual phenol.

DNA was precipitated by adding 200 µl of 5 M ammonium acetate and 800 µl 100 % ethanol and storing overnight at −20 °C. Samples were then centrifuged at 4 °C for 30 min at 16,000*g* and the supernatant discarded. DNA pellets were washed with 150 µl of cold (−20 °C) 70 % ethanol, and samples centrifuged again at 4 °C for 5 min at 16,000*g*. The supernatant was then removed, and the pelleted DNA left to air dry for 10 min before resuspension in 80 µl 10 mM Tris HCl.

### 2.4. 16S rRNA sequencing

The 16S rDNA v3- v4 region was amplified under the following PCR conditions: 341f (5'-CCTACGGGNGGCWGCAG) and 805r (5'-GACTACHVGGGTATCTAATCC) (Klindworth et al., 2013), 25 ng of template DNA, 5 pmol of each primer, and 0.5 units of Phusion Flash High-Fidelity taq polymerase mastermix (ThermoFisher Scientific) in a 25 µl reaction under the following conditions: Initial denaturation at 98 °C for 10 s, followed by 25 cycles of 98 °C for 5 s, 55 °C for 10 s, 72 °C for 30 s, and a final extension at 72 °C for 60 s.

PCR product clean-up was performed using 20 µl of AMPure XP beads (Agencourt, Beckmann Coulter) per sample, 2 × 200 µl washes of 80 % ethanol, and resuspended in 50 µl of 10 mM Tris pH 8.5 buffer. Illumina sequencing adapters (Nextera XT Index Kit, Illumina) were attached using 20 ng of template DNA, 4 µl of index primer, and 0.8 units of KAPA HiFi HotStart ReadyMix in a 40 µl reaction under the following conditions: Initial denaturation at 95 °C for 3 min, followed by 8 cycles of 95 °C for 30 s, 55 °C for 30 s, 72 °C for 30 s, and a final extension at 72 °C for 5 mins. Final PCR products were again cleaned using 56 µl of AMPure XP beads, 2 × 200 µl washes of 80 % ethanol, and resuspended in 25 µl of 10 mM Tris pH 8.5 buffer. The prepared library was pooled at a concentration of 4 nM and sequenced on a MiSeq (Illumina) using the 600-cycle MiSeq reagent kit v3 (Illumina) with a 5 % spike-in of pre-prepared PhiX sequencing control v3 library (Illumina). Sequencing was performed by the Aquatic Genomics Research Platform at the South African Institute for Aquatic Biodiversity (SAIAB, Grahamstown, South Africa). Sequence data were deposited and are publicly available in the NCBI Sequence Read Archive (SRA) under the BioProject ID PRJNA743860.

### 2.5. Bioinformatics

Bioinformatic analyses were performed using QIIME2 v2020.2 (Bolyen et al., 2019). Raw reads were filtered, trimmed and dereplicated, paired reads merged, with denoising and chimeras removed using the DADA2 pipeline (Callahan et al., 2016). Taxa were allocated to Amplicon Sequence Variants (ASVs) using the SILVA 132 database (Quast et al., 2013) using the Blast algorithm (Camacho et al., 2009) within the feature classifier plugin within QIIME2, and sequences assigned to eukaryotes and archaea were removed. There was a mean read number of 82443 across all samples, with an average of 72.1 % reads retained after denoising and chimera removal. For analysis of the photosynthetic cyanobacterial community, sequences attributed to 'Oxyphotobacteria' were extracted, and a total of 319 ASVs were allocated to the Oxyphotobacteria. Alpha diversity metrics were calculated on these sequences, with the dataset rarefied at 5740 reads, where all samples had reached the rarefaction curve plateau. Statistical tests were performed on alpha diversity metrics, and other statistics performed using JASP v0.14 (JASP Team, 2021). PCoA plots were constructed, and Analysis of compositions of microbiomes (ANCOM) (Mandal et al., 2015) performed using QIIME2, with Bray Curtis (Bray and Curtis, 1957) and weighted UniFrac (Catherine and Rob, 2005) matrices exported into PRIMER6 (Clarke and Gorley, 2006) for analysis of similarities (ANOSIM) between communities.

To identify the time when accumulation of new ASVs starts slowing down, a "piecewise regression" modelling approach was followed using the R package 'segmented' v. 1.3–4 (Muggeo, 2003, 2008). This "segmented" approach allows the user to estimate, using maximum likelihood, a breaking point (and its standard error) which splits the range of the response variable in two parts, corresponding to the ranges of values within which a linear model's parameters can take different values. This approach was employed for the study sites independently to explore potential among-site differences in the time when the dynamic of the accumulation of ASVs takes a different slope.

## 3. Results

Alpha diversity of cyanobacterial communitiesNo shells exhibited erosion degree 0, *i.e.*, an intact periostracum. Erosion rates were not uniform among sites. *Patella depressa* shells from Polzeath (mid-range) were at a more advanced stage of erosion at a younger age than shells from Shell Island and Swanage (range-edge populations) Nevertheless, erosion stage correlated positively with an increase in shell age at all three sites (Spearman's rho = Polzeath- 0.77, Shell Island- 0.72, Swanage- 0.57, all $n = 36$, $p < 0.001$; Fig. 1).

Shells from the three sites were not significantly different in age at erosion degree 1 (calcium carbonate layers exposed). Median values were Polzeath 1.49 years, Shell Island 1.47 years, Swanage 2.16 years (Kruskal-Wallis test statistic = 2.25, residual d.f. = 16, $p = 0.325$).

Bands designated erosion degree 2 (erosion of calcium carbonate layers) and erosion degree 3 (extensive erosion of calcium carbonate, exposing nacreous layers beneath) were, however, significantly younger at Polzeath than at the two range-edge sites. Median values for Polzeath, Shell Island and Swanage were 1.5, 4.08 and 4.31 years for erosion degree 2, and 4.67, 5.79 and 6.49 years for erosion degree 3 respectively (Fig. 1; Kruskal-Wallis test statistic = 12.96 and 8.04, residual d.f. 46 and 37, $p < 0.018$ for Dunn's *post-hoc* comparisons between Polzeath and the Shell Island and Swanage respectively).

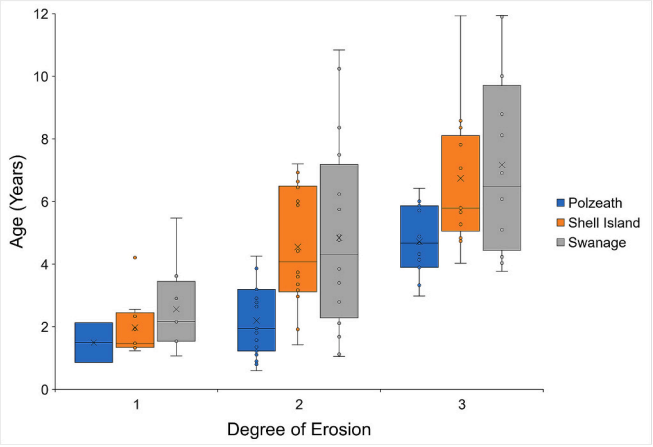


**Fig. 1.** Boxplot displaying the age (years) of sampled bands of *Patella depressa* shells from Polzeath (blue), Shell Island (orange), and Swanage (grey). Degree of erosion was coded as: 1 = periostracum eroded and calcium carbonate exposed, 2 = significant erosion of calcium carbonate layers, 3 = extensive erosion of calcium carbonate layers and underlying nacreous layers exposed. (For interpretation of the references to colour in this figure legend, the reader is referred to the web version of this article.)

All alpha diversity metrics discussed here are for photosynthetic cyanobacteria only, with the data rarefied at 5740 reads. All metrics tested (Observed ASVs, Shannon's diversity, Pielou's evenness and Faith's phylogenetic diversity) were significantly influenced by both degree of erosion and site (Table 3). Observed ASVs, diversity, evenness and phylogenetic diversity at Polzeath were all significantly lower than at Swanage, with only diversity and evenness being lower than at Shell Island (Table 4, Fig. 2). Observed ASVs, diversity and phylogenetic diversity at Shell Island were also lower than at Swanage. As erosion degree increased, there was a decrease in the values of all alpha diversity metrics. The only non-significant differences were for comparisons of phylogenetic diversity between erosion degrees 1 and 2, and between 2 and 3 (Table 4, Fig. 2D).

Segmented regression on species accumulation curves revealed that the rate of increase of ASV accumulation decreased earlier at Polzeath than Shell Island and Swanage, with breaking points of roughly 1.5, and 2.5 years (1.42+/-SE = 0.031, 2.69+/-SE = 0.205, 2.41+/-SE = 0.154), respectively for Polzeath, Shell Island, and Swanage (Fig. 3). All breaking points occurred at around 80 % of cumulative ASVs and mirrored the order in which erosion degree 2 was reached with age (Fig. 1).

### 3.1. Cyanobacterial community composition

Photosynthetic cyanobacteria formed between 65 and 80 % of the total bacterial ASVs across all treatment groups (Fig. 4), with no apparent trend among sites or degrees of erosion, although Swanage contained a slightly lower proportion of photosynthetic cyanobacteria.

**Table 3**
Kruskall-Wallis test summary for alpha diversity metrics for photosynthetic bacteria among degree of erosion and among sites *p* values displayed in brackets.

| | Observed ASVs | Shannon's diversity | Pielou's evenness | Faith's phylogenetic diversity |
|---|---|---|---|---|
| | Statistic (d.f. = 2) | Statistic (d.f. = 2) | Statistic (d.f. = 2) | Statistic (d.f. = 2) |
| Site | 27.22 (0.001) | 22.89 (0.001) | 17.15 (0.001) | 32.38 (0.001) |
| Erosion | 20.69 (0.001) | 26.96 (0.001) | 22.18 (0.001) | 10.27 (0.006) |

**Table 4**
Dunn's post-hoc tests for alpha diversity metrics among degrees of erosion (1–3) and among sites. Data displayed are *Z*-scores with p values (in brackets) after Bonferroni correction for multiple comparisons.

| | Observed ASVs | Shannon's diversity | Pielou's evenness | Faith's phylogenetic diversity |
|---|---|---|---|---|
| Polzeath, Shell Island | −0.16 (1.000) | −2.59 (0.015) | −3.15 (0.002) | −0.83 (0.614) |
| Polzeath, Swanage | −4.54 (0.001) | −4.78 (0.001) | −3.93 (0.001) | −5.24 (0.001) |
| Shell Island, Swanage | −4.45 (0.001) | −2.21 (0.041) | −0.78 (0.656) | −4.48 (0.001) |
| 1-2 | 2.94 (0.003) | 3.31 (0.001) | 2.79 (0.008) | 1.95 (0.077) |
| 2-3 | 2.19 (0.010) | 2.51 (0.018) | 2.51 (0.018) | 1.65 (0.148) |
| 1-3 | 4.57 (0.001) | 5.18 (0.001) | 4.67 (0.001) | 3.19 (0.002) |

Of the photosynthetic cyanobacteria, the two genera *Pleurocapsa* and *Phormidesmis* formed the overwhelming majority of species present.

Principle Coordinate Analysis (PCoA) plots exhibited clear definition of sites using a Bray Curtis similarity matrix (Fig. 5A), whereas, when using a weighted UniFrac matrix, sites were not as clearly delineated (Fig. 5B), suggesting that the species that drove site separation were closely related phylogenetically. Sites were significantly different from one another for both matrices across all erosion groups (Table 5). Communities of the same erosion degree appeared to cluster slightly within sites in some cases, but did not correlate with PCoA 1, 2 or 3. Differences among all levels of degree of erosion were, however, significant for both matrices, with the exception of between erosion degrees 1 and 2 for the Bray Curtis similarity matrix (Table 5).

Out of the six photosynthetic cyanobacterial ASVs that were positively correlated with an increase in erosion (Pearson correlation $p < 0.05$), none correlated significantly in more than one site. However, of the six, three belonged to the genus *Pleurocapsa* PCC-7319 (1 at each site), and two to the genus *Phormidesmis* ANT.LACV5.1 (one each at Shell Island and Polzeath), and the remaining ASV allocated only to the Nostocaceae (Swanage). Of the total 319 photosynthetic cyanobacterial ASVs, 64 correlated negatively with an increase in erosion. Analysis of compositions of microbiomes (ANCOM) also produced inconclusive results, with very few ASVs being significantly correlated with degree of erosion within or across sites.

## 4. Discussion

### 4.1. Age as an indicator of limpet erosion

The initial objective of this study was to test the hypothesis that shell age (modelled using previously determined growth curves (Oróstica et al., 2021) was significantly correlated with the degree of erosion on shells as shell age is often used to explain higher degrees of erosion (Kaehler, 1999). A significant positive correlation was observed between erosion degree and age (Fig. 1). However the relationship was not consistent across the range of *Patella depressa* in the UK, with variation similar to that observed for *Patella rustica* in the Adriatic Sea (Prusina et al., 2015). Shells at Polzeath, the centre of the host range, were eroded more quickly than those at the two range edges (Shell Island and Swanage). This trend was not reflected in the growth curves of *Patella depressa*, with individuals at the three sites displaying similar curves and maximum sizes of 30 mm after 7, 8 and 12 years for Swanage, Polzeath and Shell Island respectively (Oróstica et al., 2021). The only outstanding feature of the growth curve for Polzeath was that it had the largest theoretical maximum size, and the slowest growth rate among the three sites, possibly as a result of energy diversion to shell repair

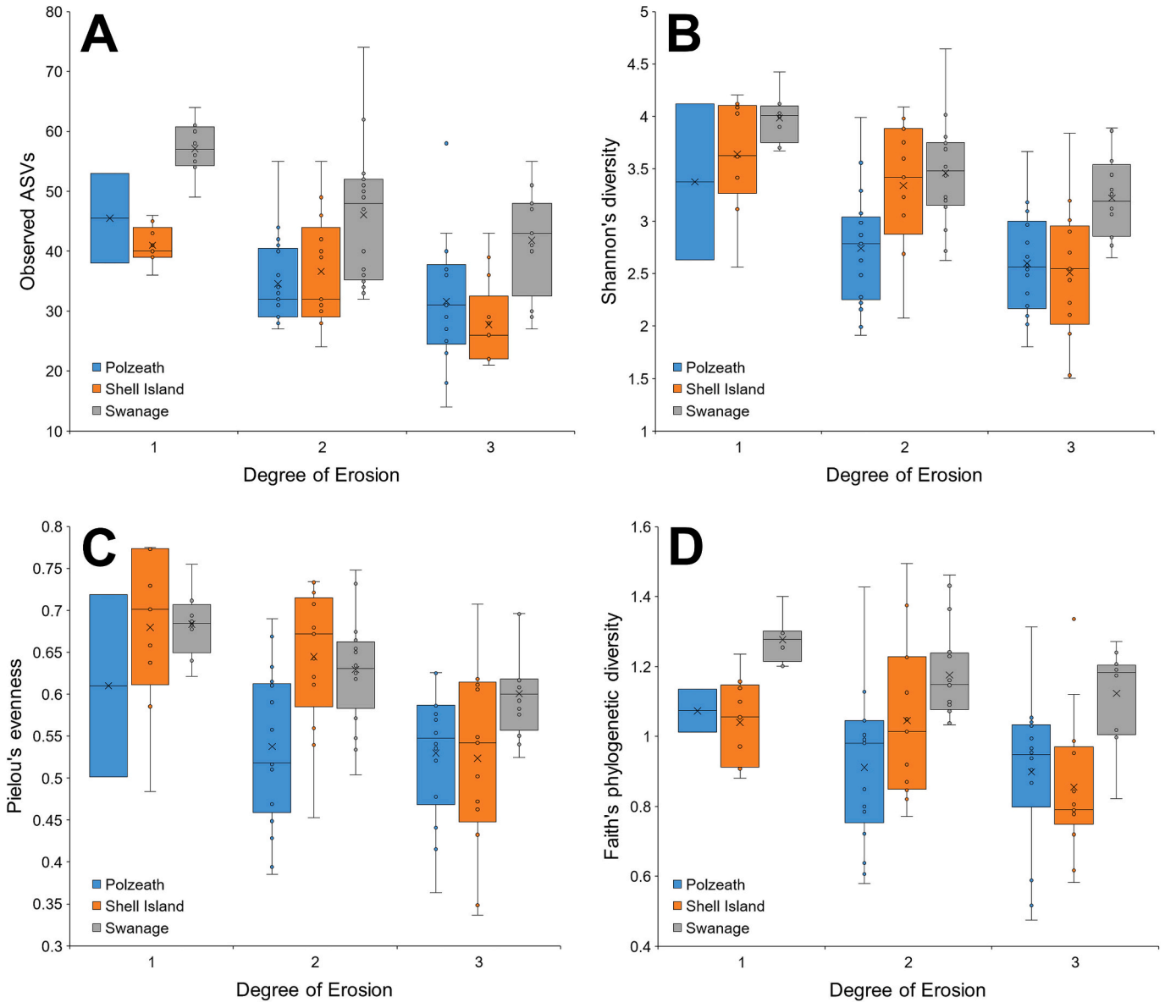


**Fig. 2.** Boxplots displaying alpha diversity metrics (A-ASV richness, B- Shannon's diversity, C- Pielou's evenness and D- Faith's phylogenetic diversity) for photosynthetic cyanobacteria and degree of erosion of sampled bands of *Patella depressa* shells from Polzeath (blue), Shell Island (orange), and Swanage (grey). Degree of erosion coded as: 1 = periostracum eroded and calcium carbonate exposed, 2 = significant erosion of calcium carbonate layers, 3 = extensive erosion of calcium carbonate layers and underlying nacreous layers exposed. (For interpretation of the references to colour in this figure legend, the reader is referred to the web version of this article.)

resulting from higher infestation levels at the site (Kaehler and McQuaid, 1999; Zardi et al., 2009; Ndhlovu et al., 2021).

Periostracum removal is essential for the euendolithic infestation of shells because a periostracum is an effective physical and chemical barrier to shell fouling (Bers et al., 2006a, 2006b, 2010), with periostracum damage accelerating the colonisation of euendolith communities (Kaehler, 1999; Ndhlovu et al., 2021). There are several explanations for the faster erosion of shells at Polzeath compared to other sites; first, shells at Polzeath may experience earlier or greater periostracum damage, for example reflecting greater suspended particle abrasion, stronger wave action, or even the effects of structure of the foreshore (*e.g.* boulders, flat rock, extensive mussel beds) (Kaehler, 1999; Ćurin et al., 2014; Alferink, 2016) on local hydrodynamics. Second, differences among sites in the degree of erosion could also reflect biological effects such as within-species or between-species differences in periostracum thickness and structure, as observed between the two mussel species *Perna perna* and *Mytilus galloprovincialis* (Zardi et al., 2009; Bers et al., 2010), the effects of grazing by other macroinvertebrates (Day et al., 2000) or even differences in the species responsible for microbial degradation (Wyness et al., 2022a, 2022b).

### 4.2. Community succession of cyanobacterial communities in vivo

The second objective was to determine if there was community succession of euendoliths *in vivo*, as observed on abiotic calcium carbonate tiles (Roush and Garcia-Pichel, 2020) and mussel shells with the periostracum artificially removed and glued to the rocky shore (Ndhlovu et al., 2020). Analysis of alpha diversity metrics of photosynthetic cyanobacteria revealed that there were significant differences across degrees of erosion, with a decrease in all metrics as erosion increased (Tables 3 & 4, Fig. 2), therefore indicating clear succession within the lithobiontic community. This contrasts with results based on morphological identification of euendolith species in mussel shells, which indicated an increase in species richness over time (Ndhlovu et al.,

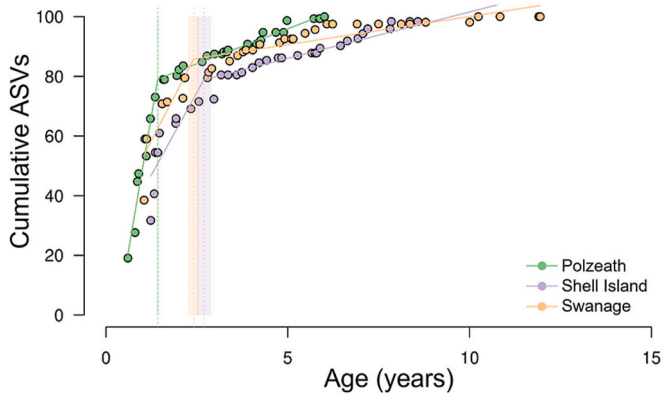


**Fig. 3.** Scatterplot of cumulative ASVs and age of sampled bands of *Patella depressa* shells from Polzeath (green), Shell Island (purple), and Swanage (orange). Segmented regression lines are fitted, with the dotted vertical lines showing the estimated breaking points (+/− standard error in shaded area). R-squared coefficients of determination = 0.99, 0.94, 0.91, respectively for Polzeath, Shell Island, and Swanage. (For interpretation of the references to colour in this figure legend, the reader is referred to the web version of this article.)

2020). Those findings were, however, based on a short timescale of 12 months, whereas the present study examined long-term community succession, rather than the early colonisation dynamics of clean substrata. In addition, the genetic approach employed here detected an order of magnitude more ASVs than the morphology-based study; indeed many of the ASVs were closely related and indistinguishable morphologically. Despite the observed increase in ASV numbers, the data did, however, indicate a decrease in phylogenetic diversity as erosion increased.

Unique sequence (ASV) accumulation with age (Fig. 3) demonstrated that there was a distinct age of shell when the rate of ASV accumulation slowed. For each site, this occurred at roughly 80 % of the total ASVs observed at each site, and the age at which this occurred coincided with the order in which the age of maximum degree of erosion took place among the sites. Polzeath reached erosion degree 2 at a median of 2 years, with the remaining sites doing so at a median of roughly 4 years. Slowing of ASV accumulation showed the same ranking at 1.42, 2.69, and 2.41 years for Polzeath, Shell Island and Swanage respectively. This indicates that the inflection point in ASV accumulation occurred after the transition from erosion degree 1 to erosion degree 2. There was, however, evidence of community succession after this degree of erosion had been reached, as alpha diversity metrics still decreased between erosion degrees 2 and 3. This occurred at shell ages of greater than 2 years for Polzeath, and 4 years for Shell Island and Swanage, suggesting that *in vivo* a climax community of cyanobacteria takes longer than this

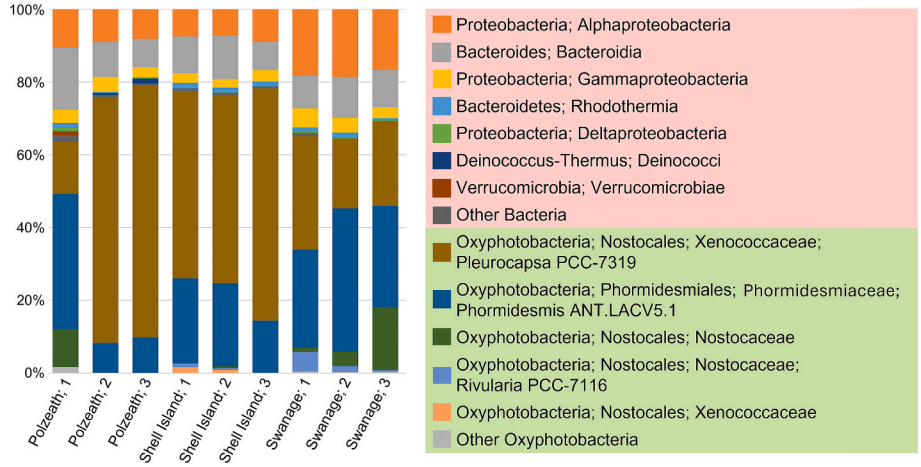


**Fig. 4.** Community composition of total bacteria for sampled bands of *Patella depressa* shells from Polzeath, Shell Island and Swanage, and degree of erosion. Degree of erosion is: 1 = periostracum eroded and calcium carbonate exposed, 2 = significant erosion of calcium carbonate layers, 3 = extensive erosion of calcium carbonate layers and underlying nacreous layers exposed. Taxa are at phylum level, with the exception of Oxyphotobacteria, which are at family or genus level. Taxa in shaded green are photosynthetic cyanobacteria, with non-photosynthetic bacteria shaded in red. (For interpretation of the references to colour in this figure legend, the reader is referred to the web version of this article.)

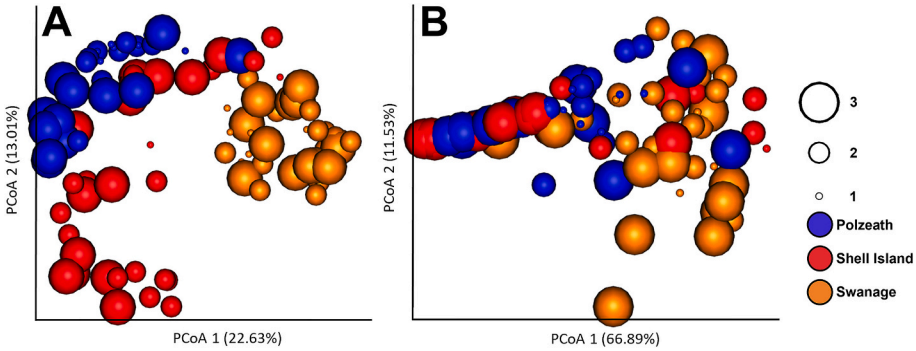


**Fig. 5.** Principle coordinates analysis plots of the beta diversity of the photosynthetic cyanobacteria communities of bands of *Patella depressa* shells from Polzeath (blue), Shell Island (red) and Swanage (orange). Plot A was constructed using a Bray Curtis similarity matrix, and plot B a weighted UniFrac matrix. Size of symbol represents degree of erosion. (For interpretation of the references to colour in this figure legend, the reader is referred to the web version of this article.)

**Table 5**
ANOSIM summary statistics for beta diversity of photosynthetic cyanobacterial communities among sites (Polzeath, Swanage, Shell Island), and degree of erosion (1,2,3).

| | | Polzeath, Swanage | Polzeath, Shell Island | Swanage, Shell Island | Site Global R | Erosion 1, 2 | Erosion 2, 3 | Erosion 1, 3 | Erosion Global R |
|---|---|---|---|---|---|---|---|---|---|
| Bray Curtis Similarity | R Statistic (*p* value) | 0.643 (0.001) | 0.31 (0.001) | 0.831 (0.001) | 0.570 (0.001) | 0.066 (0.145) | 0.107 (0.004) | 0.435 (0.001) | 0.154 (0.001) |
| Weighted Unifrac Distance | R Statistic (*p* value) | 0.500 (0.001) | 0.143 (0.006) | 0.417 (0.001) | 0.337 (0.001) | 0.151 (0.040) | 0.079 (0.018) | 0.277 (0.009) | 0.101 (0.004) |

to develop on living organisms.

Despite clear trends in the alpha diversity metrics of cyanobacterial communities, and significant differences among community compositions at difference erosion levels, there was no apparent consistent relationship between the abundance of specific taxa and the degree of erosion (Fig. 4). There was no increase in the relative abundance of photosynthetic cyanobacteria compared to the total bacterial community, and there were no obvious trends in change of abundance among taxa within the photosynthetic cyanobacterial community across all sites. Despite this, both Bray Curtis and Unifrac matrices showed significant differences in lithobiontic community composition among all sites, as well as between erosion degrees 2 and 3, further indicating that a climax community is not reached even after significant erosion of the shell over several years. Should a climax community have been reached, there would have been no significant difference among the latter stages of erosion. This suggests that the lithobiontic community continues to develop, or change, until at least shell collapse and the death of the host. For example, shell collapse due to endoliths erosion is a significant cause of mortality in mussels (Marquet et al., 2013). According to Oróstica et al. (2021), maximum growth of *P. depressa* at these sites is achieved between 4 and 10 years, and individuals of maximum size were sampled, therefore changes are not due to continuing growth of the organism, rather they may be due to continuing repair and stress response. Further studies into the community development after the time scale studied is necessary to discern whether there is indeed a climax community achieved.

### 4.3. Site specificity of endolithic community succession on Patella depressa

The third hypothesis was that changes in community composition between degrees of erosion on *Patella depressa* shells would be consistent among sites. The photosynthetic cyanobacterial communities within *P. depressa* shells were different among sites (clearest in Fig. 5A), as previously observed for several other UK calcifying organisms (Wyness et al., 2022a). There was, however, no clear trend with degree of erosion in the PCoA plots (Fig. 5). Furthermore, there were no clear trends in the changes in community composition between degrees of erosion within sites (Fig. 4). Correlations of ASVs and degree of erosion within each site (Pearson's correlation and ANCOM analysis) yielded little insight into the changes in the community with the degree of erosion, and no ASVs were consistently correlated with erosion degree across the different sites. This leads to the conclusion that community succession was not obviously consistent among sites, therefore the third hypothesis was rejected. This could be explained by models developed using epilithic biofilms where community structure and development does not follow the traditionally recognised trajectories shown for macrofauna, with microorganisms not being driven by resource-competition and niche-occupying patterns (Jackson et al., 2001). Fluctuation of micro-organismal climax communities has also been observed to be driven by small-scale temporal variation (Celussi et al., 2024), suggesting there may be no stable climax community, rather that the community continues to change with small-scale environmental variation, which in our case, could explain the among-site differences observed. Recent analysis of UK cyanobacterial communities on a variety of calcareous substrata similarly demonstrated that communities were site-specific, even within the same species although, as with the data presented here, closely related ASVs were present at the same sites (Wyness et al., 2022a).

This is similar to findings from the analysis of shells of the mussels *Perna perna* and *Mytilus galloprovincialis* across their range in southern Africa (Ndhlovu et al., 2019), with morphologically identified endolithic communities differing in composition among sites, and a decrease in richness from subtropical regions to colder water temperatures. Further work marrying morphological and sequencing data is necessary to allow comparison with earlier, morphologically-based, studies and a fuller investigation of community succession and the function of euendoliths.

## 5. Conclusion

The extent of euendolithic erosion is a good indicator of limpet age, but the relationship is site-specific, probably due to differences in the environmental factors promoting damage of the periostracum, though biological effects may also be important. *In vivo* succession in the endolith community was apparent in the alpha diversity analysis of *Patella depressa* throughout its range. This occurred on a scale of years, rather than a scale of months as previously reported for prepared abiotic substrata. Although all sites showed similar patterns in the accumulation of ASVs across time, change in the cyanobacterial community was not uniform among sites, being overwhelmed by differences in endolith community composition among them. This indicates that community succession may be site-specific, and more complex than previously thought, reflecting interactions among the biotic and abiotic drivers of endolithic colonisation. Euendolithic infestation and erosion of molluscan shells is expected to increase under changing conditions of temperature and ocean pH, but our data suggest that, like so many other effects, this may be more complex than expected and will reflect site-specific effects, as well as the nature of range-edge and central host populations.

## Data/code availability

Sequence data were deposited and are publicly available in the NCBI Sequence Read Archive (SRA) under the BioProject ID PRJNA743860.

## Authors' contribution

AW, MO and CDM contributed to the study conception and design. Material preparation, data collection and analysis were performed by AW, MO and JM. The first draft of the manuscript was written by AW and all authors commented on previous versions of the manuscript. All authors read and approved the final manuscript.

## Authors statement

Authors' Contribution: AW, MO and CMD contributed to the study conception and design.

Material preparation, data collection and analysis were performed by AW, MO and JM. The first draft of the manuscript was written by AW and all authors commented on previous versions of the manuscript. All authors read and approved the final manuscript.

## CRediT authorship contribution statement

**Adam J. Wyness:** Writing – review & editing, Writing – original draft, Methodology, Investigation, Formal analysis, Conceptualization. **Mauricio Orostica:** Writing – review & editing, Methodology, Investigation, Formal analysis, Conceptualization. **Jonathan R. Monsinjon:** Writing – review & editing, Formal analysis, Data curation. **Christopher D. McQuaid:** Writing – review & editing, Supervision, Project administration, Funding acquisition, Conceptualization.

## Ethics approval

This study was conducted in line with ethics requirements of the host institutions.

## Funding

This work is based upon research supported by the National Research Foundation of South Africa (Grant number 64801). We also acknowledge the use of infrastructure and equipment provided by the NRF-SAIAB Aquatic Genomics Research Platform and the NRF-SAIAB Institutional Support System, with special thanks to Dr. Gwynneth Matcher.

## Declaration of competing interest

The authors declare that they have no known competing financial interests or personal relationships that could have appeared to influence the work reported in this paper.

## Data availability

Sequence data were deposited and are publicly available in the NCBI Sequence Read Archive (SRA) under the BioProject ID PRJNA743860.

## References

Alferink, N., 2016. Modeling the Influence of Mussels and Oysters on Hydrodynamics and Sediment Transport. University of Twente. Master thesis. Retrieved from. https://www.utwente.nl/en/et/wem/education/mscthesis/2016/alferink.pdf.

Bers, A.V., D'Souza, F., Klijnstra, J.W., Willemsen, P.R., Wahl, M., 2006a. Chemical defence in mussels: antifouling effect of crude extracts of the periostracum of the blue mussel *Mytilus edulis*. Biofouling 22, 251–259. https://doi.org/10.1080/08927010600901112.

Bers, A.V., Prendergast, G.S., Zürn, C.M., Hansson, L., Head, R.M., Thomason, J.C., 2006b. A comparative study of the anti-settlement properties of mytilid shells. Biol. Lett. 2, 88–91 doi: Y7013122611J466L.

Bers, A.V., Díaz, E.R., da Gama, B.A., Vieira-Silva, F., Dobretsov, S., Valdivia, N., Thiel, M., Scardino, A.J., McQuaid, C.D., Sudgen, H.E., Thomason, J.C., Wahl, M., 2010. Relevance of mytilid shell microtopographies for fouling defence-a global comparison. Biofouling 26, 367–377. https://doi.org/10.1080/08927011003605888.

Bolyen, E., Rideout, J.R., Dillon, M.R., Bokulich, N.A., Abnet, C.C., Al-Ghalith, G., Alexander, H., Alm, E.J., Arumugam, M., Asnicar, F., Bai, Y., Bisanz, J.E., Bittinger, K., Brejnrod, A., Brislawn, C.J., Brown, C.T., Callahan, B.J., Caraballo-Rodríguez, A. M., Chase, J., Cope, E.K., Da Silva, R., Diener, C., Dorrestein, P.C., Douglas, G.M., Durall, D.M., Duvallet, C., Edwardson, C.F., Ernst, M., Estaki, M., Fouquier, J., Gauglitz, J.M., Gibbons, S.M., Gibson, D.L., Gonzalez, A., Gorlick, K., Guo, J., Hillmann, B., Holmes, S., Holste, H., Huttenhower, C., Huttley, G.A., Janssen, S., Jarmusch, A.K., Jiang, L., Kaehler, B.D., Kang, K.B., Keefe, C.R., Keim, P., Kelley, S. T., Knights, D., Koester, I., Kosciolek, T., Kreps, J., Langille, M.G.I., Lee, J., Ley, R., Liu, Y., Loftfield, E., Lozupone, C., Maher, M., Marotz, C., Martin, B.D., McDonald, D., McIver, L.J., Melnik, A.V., Metcalf, J.L., Morgan, S.C., Morton, J.T., Naimey, A.T., Navas-Molina, J., Nothias, L.F., Orchanian, S.B., Pearson, T., Peoples, S.L., Petras, D., Preuss, M.L., Pruesse, E., Rasmussen, L.B., Rivers, A., Robeson, M.S., Rosenthal, P., Segata, N., Shaffer, M., Shiffer, A., Sinha, R., Song, S.J., Spear, J.R., Swafford, A.D., Thompson, L.R., Torres, P.J., Trinh, P., Tripathi, A., Turnbaugh, P.J., Ul-Hasan, S., van der Hooft, J. J. J., Vargas, F., Vázquez-Baeza, Y., Vogtmann, E., von Hippel, M., Walters, Wan, Y., Wang, M., Warren, J., Weber, K.C., Williamson, C.H.D., Willis, A. D., Xu, Z.Z., Zaneveld, J.R., Zhang, Y., Zhu, Q., Knight, R., Caporaso, J.G., 2019. Reproducible, interactive, scalable and extensible microbiome data science using QIIME 2. Nat. Biotechnol. 37, 852-857. doi: https://doi.org/10.1038/s41587-019-0209-9.

Branch, G.M., 1981. The biology of limpets physical factors, energy flow, and ecological interactions. Oceanogr. Mar. Biol. Annu. Rev. 19, 235–380.

Bray, J.R., Curtis, J.T., 1957. An ordination of the upland forest communities of southern Wisconsin. Ecol. Monogr. 27, 325–349. https://doi.org/10.2307/1942268.

Callahan, B.J., McMurdie, P.J., Rosen, M.J., Han, A.W., Johnson, A.J.A., Holmes, S.P., 2016. DADA2: high-resolution sample inference from Illumina amplicon data. Nat. Methods 13, 581–583. https://www.ncbi.nlm.nih.gov/pmc/articles/PMC4927377/.

Camacho, C., Coulouris, G., Avagyan, V., Ma, N., Papadopoulos, J., Bealer, K., Madden, T.L., 2009. BLAST+: architecture and applications. BMC Bioinform. 10, 421. https://doi.org/10.1186/1471-2105-10-421.

Campbell, S.E., 1983. The modern distribution and geological history of calcium carbonate boring microorganisms. In: Westbroek, P., de Jong, E.W. (Eds.), Biomineralization and Biological Metal Accumulation: Biological and Geological Perspectives. Springer, Dordrecht, pp. 99–104. https://doi.org/10.1007/978-94-009-7944-4_8.

Campion-Alsumard, T., Hutchings, P., 1995. Microbial endoliths in skeletons of live and dead corals: *Porites lobata* (Moorea, French Polynesia). Mar. Ecol. Prog. Ser. 117, 149–157. https://doi.org/10.3354/meps117149.

Carreiro-Silva, M., Kiene, W.E., Golubic, S., McClanahan, T.R., 2012. Phosphorus and nitrogen effects on microbial euendolithic communities and their bioerosion rates. Mar. Pollut. Bull. 64, 602–613.

Catherine, L., Rob, K., 2005. UniFrac: a new phylogenetic method for comparing microbial communities. Appl. Environ. Microbiol. 71, 8228–8235. https://doi.org/10.1128/AEM.71.12.8228-8235.2005.

Celussi, M., Manna, V., Banchi, E., Fonti, V., Bazzaro, M., Flander-Putrle, V., et al., 2024. Annual recurrence of prokaryotic climax communities in shallow waters of the North Mediterranean. Environ. Microbiol. 26 (3), e16595. https://doi.org/10.1111/1462-2920.16595.

Clarke, K.R., Gorley, R.N., 2006. PRIMER v6: User manual/tutorial. PRIMER-E, Plymouth.

Couradeau, E., Roush, D., Guida, B.S., Garcia-Pichel, F., 2017. Diversity and mineral substrate preference in endolithic microbial communities from marine intertidal outcrops (Isla de Mona, Puerto Rico). Biogeosciences 14, 311–324. https://doi.org/10.5194/bg-14-311-2017.

Ćurin, M., Peharda, M., Calcinai, B., Golubić, S., 2014. Incidence of damaging endolith infestation of the edible mytilid bivalve *Modiolus barbatus*. Mar. Biol. Res. 10, 179–189. https://doi.org/10.1080/17451000.2013.814793.

Day, E.G., Branch, G.M., Viljoen, C., 2000. How costly is molluscan shell erosion? A comparison of two patellid limpets with contrasting shell structures. J. Exp. Mar. Biol. Ecol. 243, 185–208. https://doi.org/10.1016/S0022-0981(99)00120-3.

García-Escárzaga, A., Gutiérrez-Zugasti, I., González-Morales, M.R., Arrizabalaga, A., Zech, J., Roberts, P., 2020. Shell sclerochronology and stable oxygen isotope ratios from the limpet *Patella depressa* pennant, 1777: implications for palaeoclimate reconstruction and archaeology in northern Spain. Palaeogeogr. Palaeoclimatol. Palaeoecol. 560, 110023.

Garcia-Pichel, F., Ramírez-Reinat, E., Gao, Q., 2010. Microbial excavation of solid carbonates powered by P-type ATPase-mediated transcellular Ca2+ transport. Proc. Natl. Acad. Sci. USA 107, 21749–21754. https://doi.org/10.1073/pnas.1011884108.

Gektidis, M., Dubinsky, Z., Goffredo, S., 2007. Microendoliths of the shallow euphotic zone in open and shaded habitats at 30°N - Eilat, Israel - paleoecological implications. Facies 53, 43–55. https://doi.org/10.1007/s10347-006-0091-z.

Gleason, F.H., Gadd, G.M., Pitt, J.I., Larkum, A.W.D., 2017. The roles of endolithic fungi in bioerosion and disease in marine ecosystems. I. General concepts. Mycology 8, 205–215. https://doi.org/10.1080/21501203.2017.1352049.

Golubic, S., Friedmann, E.I., Schneider, J., 1981. The lithobiontic ecological niche, with special reference to microorganisms. J. Sediment. Res. 51, 475–478. https://doi.org/10.1306/212F7CB6-2B24-11D7-8648000102C1865D.

Guida, B.S., Garcia-Pichel, F., 2016. Extreme cellular adaptations and cell differentiation required by a cyanobacterium for carbonate excavation. Proc. Natl. Acad. Sci. USA 113, 5712. https://doi.org/10.1073/pnas.1524687113.

Hawkins, S.J., Moore, P.J., Burrows, M.T., Poloczanska, E., Mieszkowska, N., Herbert, R. J.H., Jenkins, S.R., Thompson, R.C., Genner, M.J., Southward, A.J., 2008. Complex interactions in a rapidly changing world: responses of rocky shore communities to recent climate change. Clim. Res. 37, 123–133.

Hogan, B., Costantini, F., Lacy, E., 1986. Manipulating the Mouse Embryo: A Laboratory Manual.

Jackson, C.R., Churchill, P.F., Roden, E.E., 2001. Successional changes in bacteria assemblage structure during epilithic biofilm development. Ecology 82 (2), 555–566.

JASP Team, 2021. JASP (Version 0.14).

Kaehler, S., 1999. Incidence and distribution of phototrophic shell-degrading endoliths of the brown mussel *Perna perna*. Mar. Biol. 135, 505–514. https://doi.org/10.1007/s002270050651.

Kaehler, S., McQuaid, C.D., 1999. Lethal and sub-lethal effects of phototrophic endoliths attacking the shell of the intertidal mussel *Perna perna*. Mar. Biol. 135, 497–503. https://doi.org/10.1007/s002270050650.

Klindworth, A., Pruesse, E., Schweer, T., Peplies, J., Quast, C., Horn, M., Glöckner, F.O., 2013. Evaluation of general 16S ribosomal RNA gene PCR primers for classical and next-generation sequencing-based diversity studies. Nucleic Acids Res. 41, e1. https://doi.org/10.1093/nar/gks808.

Langer, G., Nehrke, G., Baggini, C., Rodolfo-Metalpa, R., Hall-Spencer, J., Bijma, J., 2014. Limpets counteract ocean acidification induced shell corrosion by thickening of aragonitic shell layers. Biogeosciences 11, 7363–7368. https://doi.org/10.5194/bg-11-7363-2014.

Mandal, S., Van Treuren, W., White, R.A., Eggesbø, M., Knight, R., Peddada, S.D., 2015. Analysis of composition of microbiomes: a novel method for studying microbial composition. Microb. Ecol. Health Dis. 26, 27663. https://doi.org/10.3402/mehd.v26.27663.

Marquet, N., Nicastro, K.R., Gektidis, M., McQuaid, C.D., Pearson, G.A., Serrão, E.A., Zardi, G.I., 2013. Comparison of phototrophic shell-degrading endoliths in invasive and native populations of the intertidal mussel *Mytilus galloprovincialis*. Biol. Invasions 15, 1253–1272.

Moore, P.J., Hawkins, S.J., Thompson, R.C., 2007. Role of biological habitat amelioration in altering the relative responses of congeneric species to climate change. Mar. Ecol. Prog. Ser. 334, 11–19.

Muggeo, V., 2003. Estimating regression models with unknown break-points. Stat. Med. 22, 3055–3071. https://doi.org/10.1002/sim.1545.

Muggeo, V., 2008. Segmented: an R package to fit regression models with broken-line relationships. R News 8, 20–25.

Murphy, G.N., Perry, C.T., Chin, P., McCoy, C., 2016. New approaches to quantifying bioerosion by endolithic sponge populations: applications to the coral reefs of grand Cayman. Coral Reefs 35, 1109–1121. https://doi.org/10.1007/s00338-016-1442-z.

Ndhlovu, A., McQuaid, C.D., Nicastro, K., Marquet, N., Gektidis, M., Mobaco, C.J., Zardi, G., 2019. Biogeographical patterns of endolithic infestation in an invasive and an indigenous intertidal marine ecosystem engineer. Diversity 11, 75. https://doi.org/10.3390/d11050075.

Ndhlovu, A., McQuaid, C.D., Nicastro, K.R., Zardi, G.I., 2020. Community succession in phototrophic shell-degrading endoliths attacking intertidal mussels. J. Molluscan Stud. 87, eyaa036. https://doi.org/10.1093/mollus/eyaa036.

Ndhlovu, A., McQuaid, C.D., Monaco, C.J., 2021. Ectoparasites reduce scope for growth in a rocky-shore mussel (*Perna perna*) by raising maintenance costs. Sci. Total Environ. 753, 142020 doi:S0048-9697(20)35549-2.

Oróstica, M.H., Hawkins, S.J., Broitman, B.R., Jenkins, S.R., 2020. Performance of a warm-water limpet species towards its poleward range edge compared to a colder-water congener. Mar. Ecol. Prog. Ser. 656, 207–225.

Oróstica, M.H., Richardson, C.A., Estrella-Martínez, J., Jenkins, S.R., Hawkins, S.J., 2021. Shell growth and age determined from annual lines in the southern warm-water limpet *Patella depressa* at its poleward geographic boundaries. J. Mar. Biol. Assoc. UK 101, 707–716. https://doi.org/10.1017/S0025315421000539.

Pernice, M., Raina, J., Rädecker, N., Cárdenas, A., Pogoreutz, C., Voolstra, C.R., 2020. Down to the bone: the role of overlooked endolithic microbiomes in reef coral health. The ISME J. 14, 325–334. https://doi.org/10.1038/s41396-019-0548-z.

Pfister, C.A., Meyer, F., Antonopoulos, D.A., 2010. Metagenomic profiling of a microbial assemblage associated with the California mussel: a node in networks of carbon and nitrogen cycling. PLoS One 5, e10518. https://doi.org/10.1371/journal.pone.0010518.

Prusina, I., Peharda, M., Ezgeta-Balic, D., Puljas, S., Glamuzina, B., Golubic, S., 2015. Life-history trait of the Mediterranean keystone species *Patella rustica*: growth and microbial bioerosion. Mediterr. Mar. Sci. 16, 393–401. https://doi.org/10.12681/mms.1121.

Quast, C., Pruesse, E., Yilmaz, P., Gerken, J., Schweer, T., Yarza, P., Peplies, J., Glöckner, F.O., 2013. The SILVA ribosomal RNA gene database project: improved data processing and web-based tools. Nucleic Acids Res. 41, D590–D596. https://www.ncbi.nlm.nih.gov/pmc/articles/PMC3531112/.

Ramírez-Reinat, E.L., Garcia-Pichel, F., 2012. Characterization of a marine cyanobacterium that bores into carbonates and the redescription of the genus *Mastigocoleus*. J. Phycol. 48, 740–749. https://doi.org/10.1111/j.1529-8817.2012.01157.x.

Roush, D., Garcia-Pichel, F., 2020. Succession and colonization dynamics of endolithic phototrophs within intertidal carbonates. Microorganisms 8, 214. https://doi.org/10.3390/microorganisms8020214.

Schneider, J., Le Campion-Alsumard, T., 1999. Construction and destruction of carbonates by marine and freshwater cyanobacteria. Eur. J. Phycol. 34, 417–426. https://doi.org/10.1080/09670269910001736472.

Schönberg, C.H.L., Fang, J.K.H., Carreiro-Silva, M., Tribollet, A., Wisshak, M., 2017. Bioerosion: the other ocean acidification problem. ICES J. Mar. Sci. 74, 895–925. https://doi.org/10.1093/icesjms/fsw254.

Silva, A., Boaventura, D., Ré, P., 2003. Population structure, recruitment and distribution patterns of Patella depressa Pennant, 1777 on the central Portuguese coast. Bol. Inst. Esp. Oceanogr. 19, 461–471.

Tribollet, A., Langdon, C., Golubic, S., Atkinson, M., 2006. Endolithic microflora are major primary producers in dead carbonate substrates of Hawaiian coral reefs. J. Phycol. 42, 292–303. https://doi.org/10.1111/j.1529-8817.2006.00198.x.

Tribollet, A., Veinott, G., Dart, R., 2008. Infestation of the north American freshwater mussel *Elliptio complanata* (Head Lake, Canada) by the euendolithic cyanobacterium *Plectonema terebrans* Bornet et Flahault. Algol. Stud. 128, 65–77. https://doi.org/10.1127/1864-1318/2008/0128-0065.

Tribollet, A., Godinot, C., Atkinson, M., Langdon, C., 2009. Effects of elevated $pCO_2$ on dissolution of coral carbonates by microbial euendoliths. Glob. Biogeochem. Cycles 23. https://doi.org/10.1029/2008GB003286. GB 3008.

Wahl, M., Kröge, K., Lenz, M., 1998. Non-toxic protection against epibiosis. Biofouling 12, 205–226. https://doi.org/10.1080/08927019809378355.

Webb, S.C., Korrûbel, J.L., 1994. Shell weakening in marine mytilids attributable to blue-green-alga *Mastigocoleus* sp (Nostochopsidaceae). J. Shellfish Res. 13, 11–17.

Wyness, A.J., Oróstica, M.H., Monsinjon, J., McQuaid, C.D., 2022a. Substratum and bioregion specificity of lithobiontic communities in the rocky intertidal zone of the British Isles. Estuar. Coast. Shelf Sci. 274, 107933.

Wyness, A.J., Roush, D., McQuaid, C.D., 2022b. Global distribution and diversity of marine euendolithic cyanobacteria. J. Phycol. 58, 746–759.

Zardi, G.I., Nicastro, K.R., McQuaid, C.D., Gektidis, M., 2009. Effects of endolithic parasitism on invasive and indigenous mussels in a variable physical environment. PLoS One 4, e6560. https://doi.org/10.1371/journal.pone.0006560.